

This is a repository copy of *Dual-hop TDA-MAC and routing for underwater acoustic sensor networks*.

White Rose Research Online URL for this paper:

<https://eprints.whiterose.ac.uk/149265/>

Version: Accepted Version

---

**Article:**

Morozs, Nils [orcid.org/0000-0001-9862-7378](https://orcid.org/0000-0001-9862-7378), Mitchell, Paul Daniel [orcid.org/0000-0003-0714-2581](https://orcid.org/0000-0003-0714-2581) and Zakharov, Yuriy [orcid.org/0000-0002-2193-4334](https://orcid.org/0000-0002-2193-4334) (2019) Dual-hop TDA-MAC and routing for underwater acoustic sensor networks. *IEEE Journal of Oceanic Engineering*. pp. 865-880. ISSN 0364-9059

<https://doi.org/10.1109/JOE.2019.2933130>

---

**Reuse**

Items deposited in White Rose Research Online are protected by copyright, with all rights reserved unless indicated otherwise. They may be downloaded and/or printed for private study, or other acts as permitted by national copyright laws. The publisher or other rights holders may allow further reproduction and re-use of the full text version. This is indicated by the licence information on the White Rose Research Online record for the item.

**Takedown**

If you consider content in White Rose Research Online to be in breach of UK law, please notify us by emailing [eprints@whiterose.ac.uk](mailto:eprints@whiterose.ac.uk) including the URL of the record and the reason for the withdrawal request.

# Dual-Hop TDA-MAC and Routing for Underwater Acoustic Sensor Networks

Nils Morozs, *Member, IEEE*, Paul D. Mitchell, *Senior Member, IEEE* and Yuriy Zakharov, *Senior Member, IEEE*

**Abstract**—This paper investigates the application of underwater acoustic sensor networks (UASNs) for large scale monitoring of the ocean environment. The low propagation speed of acoustic waves presents a fundamental challenge for Medium Access Control (MAC) - coordinating the access of multiple nodes to the shared acoustic communication medium. In this paper, we propose Sequential Dual-Hop TDA-MAC (SDH-TDA-MAC) - a centralized MAC and routing protocol that facilitates efficient dual-hop scheduling in UASNs without the need for clock synchronization among the sensor nodes. BELLHOP-based simulations of a 100 node network reveal that SDH-TDA-MAC can achieve full network connectivity with 16 dB lower transmit power, compared with the single-hop TDA-MAC protocol. This provides considerable energy savings, while still providing network goodput in excess of 50% of the channel capacity. We also present a method of incorporating routing redundancy into the SDH-TDA-MAC protocol that achieves a good trade-off between the network throughput and reliability. For example, in a channel with 10% probability of link outage, incorporating double routing redundancy into SDH-TDA-MAC increases the packet delivery ratio from 81% to 95%, a significant improvement in network reliability, while still achieving the network goodput of 22% of the channel capacity, considerably higher than typical MAC protocols designed for UASNs. In summary, the high network goodput, low transmit power compared with the single-hop approach, no requirement for clock synchronization, and robust packet delivery via route diversity make SDH-TDA-MAC an efficient, reliable and practical approach to data gathering in UASNs.

**Keywords**—*Medium Access Control, Routing, Underwater Acoustic Network, Wireless Sensor Network*

## I. INTRODUCTION

The use of wireless sensor networks (WSNs) for remote monitoring of the ocean environment is becoming an increasingly popular research subject, owing to recent developments in underwater acoustic modem technologies [1]–[4]. It is investigated as a solution to a range of environmental monitoring tasks, such as water quality measurements [5], fish tracking [6], seismic monitoring [7], etc. The WSN approach to ocean monitoring provides significant advantages over the traditional deployment of data logging sensor nodes from dedicated ships, because WSNs allow flexible long term

deployments and eliminate the need to retrieve the sensor nodes from the sea bed in order to collect the data.

In contrast with terrestrial wireless communication systems, underwater radio propagation is severely limited in range due to high absorption of electromagnetic (EM) waves in seawater, and light scattering from underwater particles at optical frequencies [8]. Acoustic waves are the preferred practical medium of communication in the underwater environment; they exhibit significantly better propagation characteristics compared with EM waves. However, acoustic communications are fundamentally limited by the low sound propagation speed, approximately 1500 m/s in water, and by small bandwidth with carrier frequencies typically limited to tens of kHz, or lower for long range transmissions [8] [9]. The long propagation delays of acoustic waves present a significant challenge in Medium Access Control (MAC), i.e. coordinating transmissions of multiple acoustic communication nodes.

Many existing MAC protocols designed for underwater acoustic sensor networks (UASNs) are contention-based, where nodes access a shared channel dynamically, on demand, based on a particular set of rules [10]. These channel access rules are typically based on one or a combination of the following three principles:

- *Random access* - the nodes are allowed to transmit at random times, whenever they have a packet, i.e. based on the ALOHA principle [11]
- *Channel reservation* - before transmitting a data packet, a node must reserve channel access via dedicated control signals, typically involving a Request-to-Send (RTS), Clear-to-Send (CTS) exchange between the sender and the receiver [12] [13]
- *Carrier sensing* - a node must “listen” for the presence of other transmissions on the shared channel and only transmit a packet if the channel is idle [14].

Simple contention-based protocols such as ALOHA, ALOHA-CS or ALOHA-CA [11] can perform well in some UASN scenarios, in particular with low traffic load requirements, but generally the long propagation delays of acoustic signals render them inefficient in high throughput UASN applications due to the increased number of collisions, limited carrier sensing accuracy and higher latency in managing retransmissions. Channel reservation based protocols waste a large part of channel capacity while the nodes are waiting for control signals, e.g. RTS/CTS, acknowledgements (ACK) etc., to propagate through the slow acoustic medium to establish a communication link. These waiting times result in significant loss of throughput and poor channel utilization [9] [15] [16]. In recent work by Zhao et al. [17] the performance of multi-hop underwater acoustic networks was boosted by combining the channel reservation handshake with channel estimation to enable spatial multiplexing via

The authors are with the Department of Electronic Engineering, University of York, Heslington, York YO10 5DD, UK.

Corresponding author: Nils Morozs (nils.morozs@york.ac.uk).

This article extends the work originally published in the following conference paper: N. Morozs, P. Mitchell, and Y. Zakharov, “Unsynchronized dual-hop scheduling for practical data gathering in underwater sensor networks,” in Proceedings of the IEEE Underwater Communications and Networking Conference (UComms), 2018.

This work was supported by the UK Engineering and Physical Sciences Research Council (EPSRC) through the USMART (EP/P011975/1) and Full-Duplex (EP/R003297/1) projects.

the Time Reversal based MAC protocol (TRMAC). This is a promising cross-layer PHY-MAC approach; however, the channel utilization and packet delay improvements achieved by TRMAC are still limited by the idle times during the “probe request - probe” exchanges, and are reliant on the multipath channel diversity (i.e. low cross-correlation between the links used for simultaneous transmissions). Carrier sensing techniques are also significantly less efficient in UASNs than in terrestrial radio networks, because the carrier sensing accuracy is limited by the long propagation delays [9]. Such a dramatic change in the operating conditions, compared with terrestrial radio, necessitates the design of MAC protocols dedicated specifically to UASNs, particularly for applications with high throughput requirements.

A different class of MAC protocols, more suitable for high throughput scenarios, is based on the principle of Time Division Multiple Access (TDMA), where the nodes are scheduled to transmit their data packets in particular time slots such that the packets arrive at the intended receivers without collisions, e.g. [18]–[20]. Schedule-based MAC schemes do not involve contention for communication resources, thus removing the need for control signalling in order to establish collision-free links. Therefore, in theory, they are capable of achieving high throughput by scheduling the transmissions in a way that results in a stream of data packets separated by guard intervals at the intended receivers. For example, Lmai et al. [20] derive transmission schedules for ad hoc UASNs with linear topologies both for unicast and broadcast traffic, that maximize the network throughput. In [21] the same authors derive throughput-maximizing schedules for multi-hop grid networks, which exploit long propagation delays by allowing multiple simultaneous transmissions. Diamant and Lampe [19] propose a similar idea of exploiting long propagation delays to enable spatial time slot reuse in ad hoc networks, e.g. if two nodes transmit packets in the same time slot, it is possible for them to arrive at the receiver separately if the propagation delays are sufficiently different. A well-known schedule-based MAC protocol designed for UASNs is the Staggered TDMA Underwater MAC Protocol (STUMP) [22]. It offsets the TDMA frame timing at every node based on knowledge of their propagation delays and, thus, achieves high channel utilization. Zhuo et al. [23] propose the Delay and Queue Aware MAC protocol (DQA-MAC) which, similarly to the protocols described above, schedules concurrent transmissions based on the knowledge of the propagation delays, but also uses the packet queue information at every node to enable efficient, adaptive scheduling under variable traffic load conditions. The drawback of such coordinated scheduling protocols is their need for clock synchronization across different nodes, which can be a challenging task in UASNs due to long propagation delays, noisy time-varying multipath channels, and the signaling overhead that is not negligible compared with terrestrial radio systems [9] [24]. The use of chip-scale atomic clocks is an alternative way of providing an accurate synchronized time reference to the network nodes for long periods of time, but they are not feasible in many scenarios, in particular due to their relatively high cost, higher power consumption and ageing [25] [26]. Many of the proposed collision-free scheduling MAC protocols do not require a precise global time reference; however, their throughput performance tends to visibly deteriorate with

loose clock synchronization.

In [27] we proposed the Transmit Delay Allocation MAC (TDA-MAC) protocol, primarily designed for large scale UASNs comprising low cost, low specification sensor nodes that are currently being investigated in the EPSRC “Smart dust for large scale underwater wireless sensing (USMART)” project [28]. TDA-MAC is a schedule-based MAC protocol that is able to achieve network throughputs close to the channel capacity, but without the need for clock synchronization at the sensor nodes. However, it is limited to single-hop network topologies, where the underwater sensor nodes have a direct connection to a central surface gateway node. In [29] we proposed a TDA-MAC variant designed specifically for UASNs with fixed multi-hop line topologies; however, this type of network is mostly limited to the subsea pipeline monitoring use cases.

The purpose of this paper is to propose the Sequential Dual-Hop TDA-MAC (SDH-TDA-MAC) protocol, focusing on providing high network throughput without clock synchronization in quasi-stationary UASNs, similarly to the original TDA-MAC protocol [27], but applicable to arbitrary dual-hop network topologies. This dramatically reduces node outage due to acoustic shadows and the surface node’s limited coverage as depicted in Fig. 1, and/or improves the energy efficiency of TDA-MAC by using shorter links at lower transmit power, thus, controllably reducing the communication range of the nodes. Extending TDA-MAC to dual-hop network topologies also introduces the problem of routing, i.e. choosing which sensor nodes act as relays for other sensor nodes. Routing in UASNs is a well-established research field with many solutions available for optimizing different performance objectives, such as latency, reliability and energy efficiency [30]–[32]. However, in this paper we take a cross-layer approach by designing a routing strategy that is specifically tailored to maximizing the network throughput of the SDH-TDA-MAC protocol, i.e. a combined design of the MAC and the network layer. We believe that such cross-layer protocol design is key for achieving efficient network operation under the severe constraints imposed by the long propagation delays in UASNs.

The novel contributions of this paper are summarized below:

- *Sequential Dual-Hop TDA-MAC (SDH-TDA-MAC)* - a high throughput dual-hop scheduling protocol for large UASNs of unsynchronized sensor nodes.
- *Fewest relays routing strategy* - the problem formulation and a heuristic approximation algorithm for a throughput maximizing routing strategy designed for SDH-TDA-MAC.
- *SDH-TDA-MAC with route diversity* - a method of using dual-hop routing redundancy to greatly improve the reliability of packet delivery, similar to flooding protocols [33], but designed specifically for SDH-TDA-MAC.

The rest of the paper is organized as follows: Section II introduces the single-hop TDA-MAC protocol for centralized packet scheduling in UASNs; Section III describes the SDH-TDA-MAC protocol proposed in this paper, including the routing strategies designed specifically for SDH-TDA-MAC; Section IV evaluates the performance of the proposed MAC and routing protocol using a detailed simulation model;

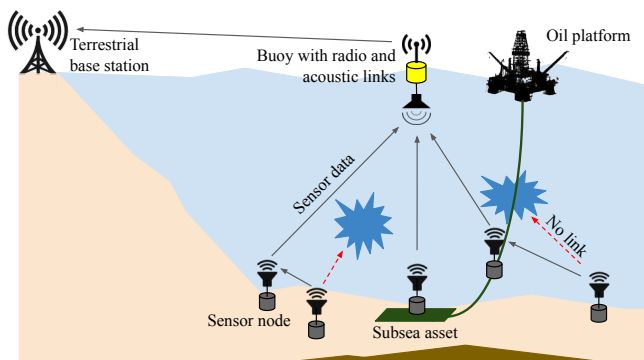


Fig. 1. Underwater wireless sensor network deployment with sensor nodes on the sea bed and a surface buoy used as the gateway node. The nodes that do not have a direct connection with the buoy, transmit their data via other sensor nodes.

finally, Section V concludes the paper.

For the reader's reference, Table I contains the list of mathematical notation used in this paper.

## II. CENTRALIZED SCHEDULING IN UASNS USING TDA-MAC

Fig. 1 shows a typical underwater WSN deployment scenario that is considered in this study. A buoy on the sea surface is used as the gateway node to gather the readings from sensor nodes deployed on the sea bed via acoustic communications, and to relay these sensor readings to an on-shore base station via a wireless radio link.

In [27] we proposed the TDA-MAC protocol for centralized scheduling of data transmissions from sensor nodes connected to a single gateway node. Its main advantage over other MAC protocols found in the literature is that it can achieve network throughputs close to the channel capacity without clock synchronization or any other advanced functionality at the sensor nodes. Therefore, it shows great potential as a practical solution for efficient data gathering in UASNs. For example, a practical application of TDA-MAC was successfully demonstrated in sea trials with a small underwater sensor network in July 2018 in Fort William, UK [34].

Fig. 2 shows a simple example of the packet flow in TDA-MAC. The gateway (master) node transmits a broadcast data request (REQ) packet that is received by every sensor node at a different time (due to large differences in propagation delays of acoustic links). Each sensor node then waits for a specific (individually assigned) amount of time before transmitting their data packet back to the gateway node. TDA-MAC also works as a general MAC protocol, regardless whether a sensor node has a packet to transmit at any particular time. The "DATA" blocks in Fig. 2 can be viewed as the time window in which a sensor node is allowed to transmit a packet, if it has anything to transmit.

The gateway node assigns a transmit delay to every individual sensor node using the following iterative equation:

$$\tau_{tx}[n] = \tau_{tx}[n-1] + \tau_{dp}[n-1] + \tau_g - 2(\tau_p[n] - \tau_p[n-1]), \quad (1)$$

where  $\tau_p[n]$  is the estimated propagation delay from the gateway node to the  $n^{\text{th}}$  sensor node,  $\tau_{tx}[n]$  is the transmit

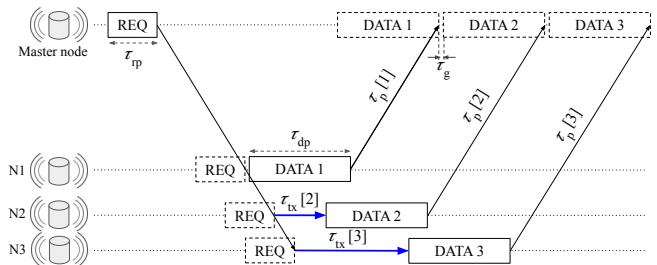


Fig. 2. TDA-MAC packet flow example, where a single gateway (master) node gathers data from 3 sensor nodes [27].

delay assigned to the  $n^{\text{th}}$  sensor node,  $\tau_{tx}[1] = 0$ , i.e. the first node starts transmitting its data packet as soon as it receives the REQ packet from the gateway node,  $\tau_{dp}[n]$  is the duration of the  $n^{\text{th}}$  node's data packet and  $\tau_g$  is the guard interval between scheduled packet receptions. The nodes in the  $\tau_{tx} = (\tau_{tx}[1], \tau_{tx}[2], \dots, \tau_{tx}[N_{sn}])$  and  $\tau_p = (\tau_p[1], \tau_p[2], \dots, \tau_p[N_{sn}])$  vectors are sorted from the shortest to the longest propagation delay from the gateway node,  $N_{sn}$  is the total number of sensor nodes. In some cases, transmit delays calculated using (1) may be negative. Then they are set to zero before continuing to iterate over the rest of the nodes in  $\tau_{tx}$ , i.e. we place the following constraint on  $\tau_{tx}[n]$ :

$$\forall n \in [1, N_{sn}], \tau_{tx}[n] \geq 0 \quad (2)$$

The key prerequisite for implementing TDA-MAC is the knowledge of propagation delays between the gateway node and every sensor node, which can be measured using a sequence of ping signals during the initial network deployment. Afterwards, during the normal operation of the network, i.e. after the initial sequence of ping signals, the gateway node can continuously monitor the accuracy of the estimated propagation delays by measuring the error in the timing of the received data packets. For example, if a data packet from a particular sensor node arrives  $\tau_{error}$  seconds later or earlier than expected, the propagation delay estimate for this node is off by  $\tau_{error}/2$ . If  $\tau_{error}$  is large enough to cause potential collisions, the gateway node can then correct the schedule by transmitting a unicast "transmit delay instruction" packet to this sensor node, and any other nodes that may need to adjust their transmission timing, as described in [27]. This approach is suitable for quasi-stationary sensor networks considered in this paper, but for networks with mobile nodes we refer the reader to a similar protocol, named APD-TDMA [35], that broadcasts the updates to every node's transmit delays on a frame-by-frame basis.

The guard interval  $\tau_g$  is an important design parameter that is used to separate consecutive data packets received at the gateway node. It should be long enough to avoid packet collisions due to inaccuracies in propagation delay estimates, slow variations in node positions and the multipath channel delay spread. However, extending the guard interval also increases the amount of idle time on the channel and, thus, reduces the throughput and increases the latency. Therefore, the length of the guard interval should be specifically chosen for a given network deployment and underwater acoustic environment, taking into account the network size, the link lengths, the expected node drift, the reflectivity of the sea surface and bottom, the robustness of the physical layer against multipath,

TABLE I. MATHEMATICAL NOTATION

Term	Description
$\tau_p[n]$	Propagation delay between master node and node $n$ in single-hop TDA-MAC
$\tau_{tx}[n]$	Transmit delay assigned to node $n$ in single-hop TDA-MAC
$\tau_{dp}[n]$	Duration of the data packet transmitted by node $n$
$\tau_{rp}$	Duration of the data request (REQ) packet
$\tau_g$	Duration of the guard interval
$N$	Total number of nodes, including the gateway node
$N_{sn}$	Total number of sensor nodes
$C$	Binary connectivity matrix $[N \times N]$ (the index of the gateway node is 1)
$R$	Binary routing matrix $[N \times N]$ (if $R[i, j] = 1$ , node $j$ transmits data packets to node $i$ )
$T_p$	Propagation delay matrix $[N \times N]$
$T_{tx}$	Transmit delay matrix (SDH-TDA-MAC schedule) $[N \times N]$
$T_p[i, j]$	Propagation delay between node $i$ and node $j$
$T_{tx}[i, j]$	Transmit delay assigned to node $j$ by node $i$
$M_{dual-hop}$	Set of nodes that require a dual-hop connection to the gateway
$M_{relays}$	Set of nodes that act as relays for other sensor nodes
$\hat{M}_{relays}$	Set of relay nodes in the fewest relays routing strategy
$\hat{M}_{relays}^{red}$	Set of relay nodes used for routing redundancy in the fewest relays routing strategy
$M_{direct}$	Set of non-relay nodes directly connected to the gateway node
$M_{children}^i$	Set of sensor nodes connected via relay node $i$
$r_i$	Index of the relay node assigned to node $i$
$\tau_{sf}[i]$	Duration of the TDA-MAC subframe where node $i$ is the master node
$\tau_{req}$	Interval between consecutive REQ packet transmissions in SDH-TDA-MAC

etc. A detailed study on the appropriate selection of the guard interval is beyond the scope of this paper, but is part of our future work that involves testing a range of guard intervals in lake and sea trials. In this paper we use a 100 ms guard interval which could tolerate approximately 150 m changes in relative node positions (assuming 1,500 m/s sound speed and low multipath propagation) before the transmit delays have to be adjusted to compensate for the drift.

Another parameter that needs to be established by the gateway node is the regularity (i.e. the period) of the TDA-MAC frames, during which every sensor node gets an opportunity to transmit a data packet, i.e. the time between the start of the first transmission and the end of the last reception at the master node in Fig. 2. This frame period is specific to any given application depending on how frequently the sensor readings need to be gathered. However, there is a constraint on the minimum frame period that depends on the propagation delays in the network. This constraint is given by:

$$\tau_{frame} \geq \max_n \{2\tau_p[n] + \tau_{tx}[n] + \tau_{dp}[n]\} + \tau_{rp}, \quad (3)$$

where  $\tau_{rp}$  is the duration of the REQ packet, and  $\tau_{frame}$  is the frame period, i.e. the time interval between two consecutive REQ packet transmissions. The above expression states that the gateway node cannot transmit the REQ packet for the next frame before it finishes receiving a data packet from the last sensor node.

To summarize, TDA-MAC is a centralized single-hop MAC protocol that achieves highly efficient use of channel capacity and provides fair round robin access to all connected sensor nodes.

### III. SEQUENTIAL DUAL-HOP TDA-MAC

The main disadvantage of TDA-MAC described in the previous section is that it requires a centralized single-hop topology, which cannot accommodate nodes outside of coverage of the gateway node, e.g. due to acoustic shadows or if a sensor node is out of range of the gateway node.

In this section we propose Sequential Dual-Hop TDA-MAC (SDH-TDA-MAC), an extension of TDA-MAC, that combines it with dual-hop routing, where the sensor nodes without a direct link to the gateway node communicate via TDA-MAC with other sensor nodes that act as relays.

#### A. Dual-Hop Routing

First, the links between the gateway node and all in-range sensor nodes, and the links between the relay nodes and out-of-coverage sensor nodes, need to be established via the network discovery and localization processes, including the propagation delay estimation for every link. This typically involves a series of ping packets, where the delay between sending a ping packet and receiving a response is used to estimate the propagation delay on that link, e.g. as demonstrated in sea trials in [34]. The implementation of these

network setup functions are out of the scope of this paper. However, there are a number of algorithms proposed in the literature that can achieve this goal, e.g. in [36]–[38]. In quasi-stationary sensor networks considered in this paper this process will not have to be repeated often to maintain a relatively accurate estimate of the network topology. Furthermore, the TDA-MAC guard intervals are designed to tolerate inaccuracies in propagation delay estimates used for scheduling.

Fig. 3 shows an illustrative example of dual-hop routing. In this scenario 20 sensor nodes are spread across a  $6 \times 6$  km<sup>2</sup> area at roughly 500 m depth. Since 7 out of 20 nodes are outside of the gateway node’s coverage, they send their sensor data via other nodes that do have direct connections to the gateway. The TDA-MAC protocol described in Section II is used at two levels of hierarchy - between the gateway and directly connected sensor nodes, and between every relay node and the child nodes in their branch, as explained further in Subsection III-E. In this way, the network exploits the many-to-one connections to increase the throughput, whereas every relay branch of the network topology is processed sequentially, increasing the idle time caused by the dual-hop round trip delays and thus reducing the throughput. Therefore, to maximize the throughput of the SDH-TDA-MAC protocol, the routing strategy should minimize the number of relay nodes, hereafter referred to as “fewest relays” routing. For example, Fig. 3 shows an example of the fewest relays routing strategy, where the routes are chosen such that there are only two relay nodes, in this case the smallest possible number of relays. The fewest relays routing strategy for UASNs running SDH-TDA-MAC was initially investigated in [39], and was shown to achieve significantly higher network throughput than the minimum delay routing strategy.

### B. Fewest Relays Routing

The fewest relays routing table is derived by the gateway node as follows.

Let  $C$  be an  $N \times N$  connectivity matrix, where  $N = N_{sn} + 1$  is the total number of nodes, including 1 gateway node and  $N_{sn}$  sensor nodes, and the index of the gateway node is 1. The elements of  $C$  are defined as follows:

$$C[i, j] = \begin{cases} 0, & i = j \\ 1, & \text{there is a link between } i \text{ and } j \\ 0, & \text{there is no link between } i \text{ and } j \end{cases} \quad (4)$$

We assume that the connectivity matrix  $C$  and a matrix of propagation delays on every link  $T_p$  are established during the network discovery and setup stage, and are then periodically updated based on the delays of received data packets, if necessary. This process is sufficient to maintain an accurate schedule in a quasi-stationary underwater sensor network.

We can identify the set of sensor nodes  $M_{\text{dual-hop}}$ , that do not have a direct link with the gateway and, therefore, require a dual-hop connection, as follows:

$$M_{\text{dual-hop}} = \{n \mid C[1, n] = 0\} \quad (5)$$

The aim of the routing algorithm is to find the smallest set  $\hat{M}_{\text{relays}}$  that provide dual-hop connections to all nodes in  $M_{\text{dual-hop}}$ . This optimization problem can be formulated as

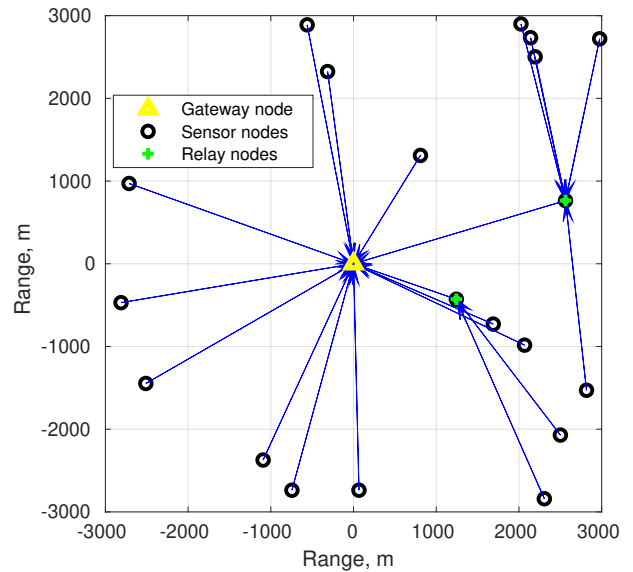


Fig. 3. Example of dual-hop routing used in conjunction with Sequential Dual-Hop TDA-MAC in a network of 20 sensor nodes at approx. 500 m depth with 3 km communication range. The sensor nodes outside of the gateway node’s coverage send their data via other sensor nodes. TDA-MAC is used by the gateway node to gather data from all directly connected sensor nodes, and by every relay sensor node gathering data within its network branch.

follows:

$$\text{Minimize } |\hat{M}_{\text{relays}}|, \quad (6)$$

where  $|\cdot|$  is the cardinality of a set, such that (s.t.):

$$\forall i \in M_{\text{dual-hop}}, \exists j \in \hat{M}_{\text{relays}}, C[1, j] = 1 \wedge C[j, i] = 1, \quad (7)$$

This is a set cover problem [40]. Every potential relay node  $j$  can be represented by a set of nodes directly linked to it:  $M_C^j = \{i \mid C[j, i] = 1\}$ . The optimal set of relay nodes  $\hat{M}_{\text{relays}} = \{a, b, \dots\}$  is determined by finding the smallest collection of node sets  $\mathcal{S} = \{M_C^a, M_C^b, \dots\}$  such that their union contains all nodes in  $M_{\text{dual-hop}}$ :

$$M_{\text{dual-hop}} \subseteq \bigcup_{M_C^j \in \mathcal{S}} M_C^j, \quad (8)$$

i.e. this is a problem of finding the set cover  $\mathcal{S}$  of  $M_{\text{dual-hop}}$  that uses the smallest number of sets  $M_C^j$ .

The set cover problem is NP-hard [40]; therefore, an exact computationally efficient method of finding the optimal set of relays  $\hat{M}_{\text{relays}}$  does not exist. Instead, it can be found by a heuristic approximation algorithm that does not guarantee an optimal solution but efficiently finds good suboptimal solutions.

Algorithm 1 gives details of an algorithm we propose for finding the smallest set of relay nodes for this routing problem. However, the general approximation algorithms for the set cover problem can also be used to solve it, e.g. see [41], [42]. Our proposed algorithm iterates over every unconnected node in  $M_{\text{dual-hop}}$  and chooses a relay node for it with a bias towards the nodes that are already acting as a relay. The solution produced by this procedure depends on the order in which it iterates over the nodes in  $M_{\text{dual-hop}}$ ; therefore, it is repeated multiple times with different random



orders of nodes in  $M_{\text{dual-hop}}$ , always keeping track of the best solution. For example, in our Matlab implementation, we limited the number of times this procedure is repeated to 10000 which increases the likelihood of finding a good solution, whilst keeping the computation time low.

**Algorithm 1** Iterative approximation algorithm for solving the fewest relays routing problem

---

```

1: Initialize  $\hat{N}_{\text{relays}} = \infty$ 
2: for large number of iterations (e.g.  $10^4$ ) do
3:   Initialize  $N_{\text{relays}} = 0$  and  $M_{\text{relays}} = \emptyset$ 
4:   Let vector  $\mathbf{m}_{\text{dh}}$  be a random permutation of  $M_{\text{dual-hop}}$ 
5:   for every node  $i$  in  $\mathbf{m}_{\text{dh}}$  do
6:     Create a set of possible relays for this node:
        $M_r^i = \{j \mid C[1, j] = 1, C[j, i] = 1\}$ 
7:     if  $M_r^i \neq \emptyset$  then
8:       Find nodes already used as relays:
        $M_r^{i*} = M_r^i \cap M_{\text{relays}}$ 
9:       if  $M_r^{i*} \neq \emptyset$  then
10:        Choose relay node  $r_i$  randomly out of  $M_r^{i*}$ 
11:       else
12:        Choose relay node  $r_i$  randomly out of  $M_r^i$ 
13:         $M_{\text{relays}} \leftarrow \{M_{\text{relays}}, r_i\}$ ;  $N_{\text{relays}} \leftarrow N_{\text{relays}} + 1$ 
14:       end if
15:     end if
16:   end for
17:   if  $N_{\text{relays}} < \hat{N}_{\text{relays}}$  then
18:     Update the best solution:  $\hat{M}_{\text{relays}} = M_{\text{relays}}$ 
19:      $\hat{N}_{\text{relays}} = N_{\text{relays}}$ 
20:   end if
21: end for
22: Return the best solution:  $\hat{M}_{\text{relays}}$ 

```

---

Table II compares solutions found by our proposed heuristic algorithm with those produced by the classical greedy set cover approximation algorithm [42], which iteratively chooses a relay node that maximizes the number of unconnected nodes it covers, until all nodes in  $M_{\text{dual-hop}}$  are covered. The values in Table II show the percentage of simulation trials where our algorithm performed better (i.e. the solution contained fewer relay nodes), the same (same number of relay nodes) and worse (more relay nodes). We ran 10000 simulation trials for each network size (20/50/100 nodes + 1 gateway node) using random connectivity matrices with an equal 50/50 likelihood of a link between any pair of nodes. In the majority of the cases both algorithms produce equally good solutions; however, in other cases, our proposed algorithm almost always produces better solutions. In particular, the benefit of the proposed heuristic algorithm is more pronounced for large network sizes, e.g. finding better solutions in 20% of 100-node networks.

After the set of relay nodes  $\hat{M}_{\text{relays}}$  is identified via Algorithm 1, a relay node  $r_i$  is chosen, for every sensor node that requires a dual-hop connection, that minimizes the total propagation delay across two hops (sensor-relay and relay-gateway):

$$\forall i \in M_{\text{dual-hop}}, \quad r_i = \arg \min_{j \in \hat{M}_{\text{relays}}} \{T_p[j, i] + T_p[1, j]\} \quad (9)$$

$$\text{s.t. } C[1, j] = 1 \wedge C[j, i] = 1$$

TABLE II. PERFORMANCE OF THE PROPOSED FEWEST RELAYS ROUTING ALGORITHM COMPARED WITH THE GREEDY SET COVER APPROXIMATION ALGORITHM

Network size	% of simulations		
	Better	Same	Worse
20 nodes	8.5%	91.5%	0%
50 nodes	10.6%	89.4%	0%
100 nodes	20.4%	79.5%	0.1%

Now, having identified all single-hop and dual-hop connections, a binary routing matrix  $\mathbf{R}$  is constructed as follows. First, it is initialized as an  $N \times N$  matrix of zeros:

$$\forall i, j \in [1, N], R[i, j] = 0 \quad (10)$$

Then, all direct connections between the gateway and sensor nodes are recorded by copying the first row of the connectivity matrix into the first row of the routing matrix, i.e. all nodes that have a direct link with the gateway, transmit the data directly to it:

$$\forall i \in [2, N], R[1, i] = C[1, i] \quad (11)$$

Finally, all dual-hop connections are recorded by setting the elements of  $\mathbf{R}$  corresponding to the links between the sensor nodes (columns) and their assigned relays (rows) to 1:

$$\forall i \in M_{\text{dual-hop}}, R[r_i, i] = 1 \quad (12)$$

This routing matrix is derived centrally at the gateway node which keeps track of the entire network topology. In contrast, the sensor nodes are required to store only small parts of this routing matrix - the IDs of the nodes for which they act as a relay (if any), and the ID of the node to which they have to send the data (either the gateway or a relay node).

### C. Dual-Hop Routing with Redundancy

Although the dual-hop routing approach described above is highly efficient in terms of network throughput [43], it makes the network vulnerable to link failures and packet loss, common in the harsh underwater acoustic environment. For example, if a link between a particular sensor node and the gateway node fails, e.g. due to acoustic noise, obstructed signal path or multipath fading, in the best case it will result in the loss of one data packet, but in the worst case - in the loss of sensor data from an entire branch of the network, if this sensor node is a relay.

We propose a method of incorporating routing redundancy into our SDH-TDA-MAC protocol to increase the network's resilience to distributed link failures and, therefore, improve the reliability of packet delivery. Fig. 4 shows an example of this routing strategy, using the same network topology as was shown in Fig. 3. In this setup every sensor node has two unique paths to send a data packet to the gateway node, i.e. there is a set of primary routes and a redundant set of secondary routes whose purpose is to introduce route diversity and increase the network reliability. The primary set of routes is derived using the approach described in the previous subsection, while a redundant set of routes is derived as follows.

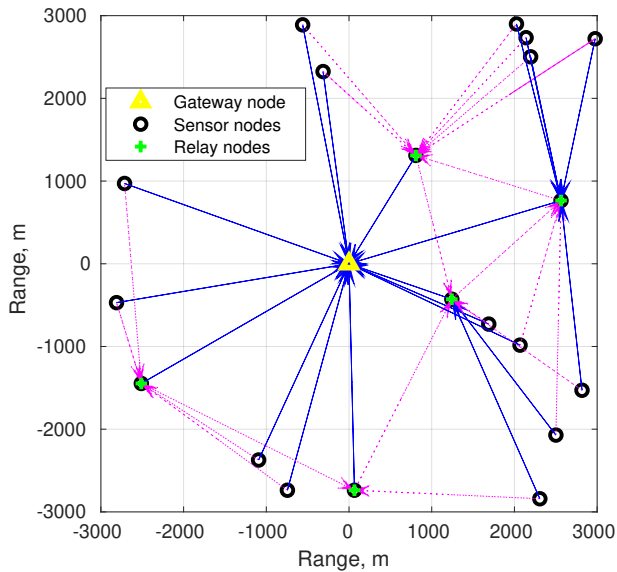


Fig. 4. Dual-hop routing with double redundancy in a network of 20 sensor nodes at approx. 500 m depth with 3 km communication range. Every sensor node has two different scheduled routes of delivering a single data packet to increase the network resilience to random link failures.

The set of relays for the redundant routes  $\hat{M}_{\text{relays}}^{\text{red}}$  must satisfy the following criteria:

$$\begin{aligned} \forall i \in [2, N], \exists j \in \hat{M}_{\text{relays}}^{\text{red}}, \\ C[1, j] = 1 \wedge C[j, i] = 1 \wedge R[j, i] \neq 1 \wedge R[i, j] \neq 1. \end{aligned} \quad (13)$$

Here, the secondary relay selection has an additional pair of constraints compared with the primary relay set selection described by (6). Constraint  $R[j, i] \neq 1$  ensures that the sensor nodes find a new relay path if available. Constraint  $R[i, j] \neq 1$  prevents the nodes from reversing an existing relay path, i.e. if node  $j$  is a relay for node  $i$ , node  $i$  cannot be a relay for node  $j$ .

In line with the fewest relays routing strategy proposed above,  $\hat{M}_{\text{relays}}^{\text{red}}$  is chosen that minimizes the number of relays in both the primary and the redundant route sets. Therefore, this extends the original routing problem from Subsection III-B as follows:

$$\text{Minimize } \left| \hat{M}_{\text{relays}} \cup \hat{M}_{\text{relays}}^{\text{red}} \right|, \text{ s.t. (7) } \wedge \text{(13)} \quad (14)$$

The solution to (14) cannot be found using a general set cover approximation algorithm, since the redundant relay node selection does not only involve finding the smallest set  $\hat{M}_{\text{relays}}^{\text{red}}$  covering all sensor nodes  $i \in [2, N]$ , but also finding a corresponding valid routing matrix  $\hat{R}$  that satisfies the additional constraints in (13). Therefore, we extend our heuristic relay node selection algorithm, that was shown to outperform the greedy set cover approximation algorithm in Subsection III-B, and propose Algorithm 2 for adding routing redundancy whilst conforming to the fewest relays routing strategy.

The process in Algorithm 2 is repeated for every additional level of redundancy required. Algorithm 3 summarizes the whole dual-hop routing algorithm.

---

#### Algorithm 2 Adding routing redundancy to the fewest relays routing algorithm

---

- 1: Start with the current  $\hat{M}_{\text{relays}}$  and  $R$
  - 2: Initialize  $\hat{N}_{\text{relays}} = \infty$
  - 3: **for** large number of iterations (e.g.  $10^4$ ) **do**
  - 4: Initialize the redundant set of relays  $M_{\text{relays}}^{\text{red}} = \emptyset$  and temporary routing matrix  $R_{\text{temp}} = R$
  - 5: Initialize  $N_{\text{relays}} = |\hat{M}_{\text{relays}}|$
  - 6: Let vector  $m_{\text{sn}}$  be a random permutation of  $[2, N]$
  - 7: **for** every node  $i$  in  $m_{\text{sn}}$  **do**
  - 8: Find the set of eligible relays:  $M_r^i = \{j \mid C[1, j]=1, C[j, i]=1, R_{\text{temp}}[j, i]=0, R_{\text{temp}}[i, j]=0\}$
  - 9: **if**  $M_r^i \neq \emptyset$  **then**
  - 10: Find nodes already used as relays:  $M_r^{i*} = M_r^i \cap (M_{\text{relays}}^{\text{red}} \cup \hat{M}_{\text{relays}})$
  - 11: **if**  $M_r^{i*} \neq \emptyset$  **then**
  - 12: Choose relay node  $r_i$  randomly out of  $M_r^{i*}$
  - 13: **else**
  - 14: Choose relay node  $r_i$  randomly out of  $M_r^i$
  - 15:  $M_{\text{relays}}^{\text{red}} \leftarrow \{M_{\text{relays}}^{\text{red}}, r_i\}; N_{\text{relays}} \leftarrow N_{\text{relays}} + 1$
  - 16: **end if**
  - 17: Update:  $R_{\text{temp}}[r_i, i] = 1$
  - 18: **end if**
  - 19: **end for**
  - 20: **if**  $N_{\text{relays}} < \hat{N}_{\text{relays}}$  **then**
  - 21: Update solution:  $\hat{R} = R_{\text{temp}}, \hat{M}_{\text{relays}}^{\text{red}} = M_{\text{relays}}^{\text{red}}$
  - 22:  $\hat{N}_{\text{relays}} = N_{\text{relays}}$
  - 23: **end if**
  - 24: **end for**
  - 25: Update the set of relay nodes:  $\hat{M}_{\text{relays}} = (\hat{M}_{\text{relays}}^{\text{red}} \cup \hat{M}_{\text{relays}})$
  - 26: Return the best solution:  $\hat{R}, \hat{M}_{\text{relays}}$
- 

---

#### Algorithm 3 Dual-hop routing with redundancy designed for SDH-TDA-MAC

---

- 1: Do network discovery to derive the connectivity and propagation delay matrices,  $C$  and  $T_p$
  - 2: Initialize the routing matrix  $R$  using (10) and (11)
  - 3: Identify the nodes that require a dual-hop connection  $M_{\text{dual-hop}}$ , using (5)
  - 4: Find relay nodes  $\hat{M}_{\text{relays}}$  that solve (6) subject to (7)
  - 5: **for** every sensor node  $i \in M_{\text{dual-hop}}$  **do**
  - 6: Find its best relay node using (9)
  - 7: Update the routing matrix  $R$  using (12)
  - 8: **end for**
  - 9: **for** every additional level of redundancy **do**
  - 10: Create a routing matrix  $\hat{R}$  with additional routes for every node using Algorithm 2
  - 11: Update the routing matrix  $R = \hat{R}$
  - 12: **end for**
-



#### D. Transmit Delay Allocation

SDH-TDA-MAC involves single-hop TDA-MAC data gathering at the gateway node and every relay node. Therefore, to enable transmit delay allocation at these two levels of hierarchy, instead of a transmit delay vector  $\tau_{tx}$  used in single-hop TDA-MAC, a transmit delay matrix  $\mathbf{T}_{tx}$  is used:

$$\mathbf{T}_{tx} = \begin{bmatrix} \emptyset & T_{tx}[1, 2] & T_{tx}[1, 3] & \cdots & T_{tx}[1, N] \\ \emptyset & \emptyset & T_{tx}[2, 3] & \cdots & T_{tx}[2, N] \\ \emptyset & T_{tx}[3, 2] & \emptyset & \cdots & T_{tx}[3, N] \\ \vdots & \vdots & \vdots & \ddots & \vdots \\ \emptyset & T_{tx}[N, 2] & T_{tx}[N, 3] & \cdots & \emptyset \end{bmatrix}, \quad (15)$$

where  $\emptyset$  denotes the elements of  $\mathbf{T}_{tx}$  that are never used. Each row of  $\mathbf{T}_{tx}$  corresponds to a node that performs data gathering, with the first row reserved for the gateway node. For example, if node  $i$  acts as the relay for sensor nodes  $j$  and  $k$ , then the transmit delays assigned to the nodes  $j$  and  $k$  are stored in  $T_{tx}[i, j]$  and  $T_{tx}[i, k]$  respectively. The first column of  $\mathbf{T}_{tx}$  is unused, because the gateway node does not transmit any data packets, but only receives them.

To allocate transmit delays, first, the sensor nodes with a direct link to the gateway are split into two sets - relay nodes  $M_{relays}$  and direct non-relay nodes  $M_{direct}$ :

$$M_{relays} = \left\{ n \mid n \in [2, N], \left( \sum_i R[n, i] \right) > 0 \right\} \quad (16)$$

$$M_{direct} = \left\{ n \mid n \in [2, N], R[1, n] = 1, \left( \sum_i R[n, i] \right) = 0 \right\} \quad (17)$$

Then, single-hop TDA-MAC introduced in Section II is employed to allocate transmit delays to the direct non-relay nodes. A vector of propagation delays  $\tau_p$  between the gateway node and each direct non-relay node is extracted as follows:

$$\tau_p = \left\{ t \mid t \in T_p[1, n], \forall n \in M_{direct} \right\} \quad (18)$$

The vector  $\tau_p$  is then used as the input to the single-hop TDA-MAC transmit delay allocation algorithm described by the iterative formula in (1). It returns a vector of transmit delays  $\tau_{tx}$  for every node represented in  $\tau_p$ . Now, the derived transmit delays are recorded in the corresponding elements of the first row of the transmit delay matrix as follows:

$$\forall m \in M_{direct}, T_{tx}[1, m] = \tau_{tx}[j] \quad (19)$$

where  $j$  is the index of node  $m$  in the transmit delay vector  $\tau_{tx}$ .

A similar procedure is followed to allocate transmit delays within every relay branch of the network, i.e. between one or several sensor nodes connected to the same relay node.

Let  $i$  be the index of a relay node. The set of sensor nodes connected to it, referred to as its "children", is identified as follows:

$$M_{children}^i = \left\{ m \mid m \in [2, N], R[i, m] = 1 \right\} \quad (20)$$

Single-hop TDA-MAC scheduling is then applied to this set of nodes in a similar way to that shown in (18) and (19). First, a propagation delay vector is extracted as follows:

$$\tau_p = \left\{ t \mid t \in T_p[i, n], \forall n \in M_{children}^i \right\} \quad (21)$$

Then, the resulting single-hop TDA-MAC delays  $\tau_{tx}$  are embedded into  $\mathbf{T}_{tx}$  as follows:

$$\forall m \in M_{children}^i, T_{tx}[i, m] = \tau_{tx}[j] \quad (22)$$

where  $j$  is the index of node  $m$  in the transmit delay vector  $\tau_{tx}$ . Note that this time the  $i^{\text{th}}$  row of  $\mathbf{T}_{tx}$  represents the relay node  $i$ .

The SDH-TDA-MAC scheduling procedure that calculates the transmit delay matrix is summarized in Algorithm 4.

---

#### Algorithm 4 Calculation of the transmit delay matrix in Sequential Dual-Hop TDA-MAC

---

- 1: Initialize  $\mathbf{T}_{tx}$  as an  $N \times N$  matrix of zeros
  - 2: Extract propagation delay vector of single-hop non-relay nodes using (18)
  - 3: Calculate TDA-MAC delay vector  $\tau_{tx}$  using (1)
  - 4: Update  $\mathbf{T}_{tx}$  using (19)
  - 5: **for** every relay node  $i \in M_{relays}$  **do**
  - 6:   Identify its child nodes  $M_{children}^i$  using (20)
  - 7:   Extract propagation delay vector of the child nodes using (21)
  - 8:   Calculate TDA-MAC delay vector  $\tau_{tx}$  using (1)
  - 9:   Update  $\mathbf{T}_{tx}$  using (22)
  - 10: **end for**
- 

#### E. The Sequential Dual-Hop TDA-MAC Protocol

After all the links and their propagation delays are established, and the transmit delay matrix  $\mathbf{T}_{tx}$  is derived, the network employs the SDH-TDA-MAC protocol to enable wireless data gathering from the underwater sensor nodes, as described by the flowcharts in Fig. 5.

The gateway node first broadcasts the REQ packet, giving all directly connected non-relay sensor nodes an opportunity to transmit their data in their allocated times, using the TDA-MAC protocol described in Section II. It then queries every relay node's branch of the network sequentially. When a relay node receives a unicast REQ packet addressed specifically to it, it also employs TDA-MAC to enable its child nodes to transmit data, if they have any packets to transmit. It then forwards any packets it received, together with its own data packet, to the gateway node. If a sensor node receives a broadcast REQ packet, it can transmit a data packet after its allocated delay, only if the source address of the REQ packet is its assigned next hop destination in the routing matrix. For example, if node  $j$  receives a broadcast REQ packet from node  $i$ , node  $j$  can only respond with a data packet if  $R[i, j] = 1$ . The SDH-TDA-MAC implementation at the sensor node, incorporating both relay and non-relay functionality, is shown in Fig. 5b.

A key task of the gateway node is to schedule the upcoming REQ packets appropriately, taking into account an accurate estimate of the length of time during which it expects to receive data packets in response to its previous REQ. This enables SDH-TDA-MAC to be used as a general schedule-based MAC protocol, where the REQ packet transmissions are used for distributing a local timing reference, and sensor nodes may or may not choose to transmit data packets, depending on the application and the type of traffic driving the sensor nodes. It also makes the network more robust

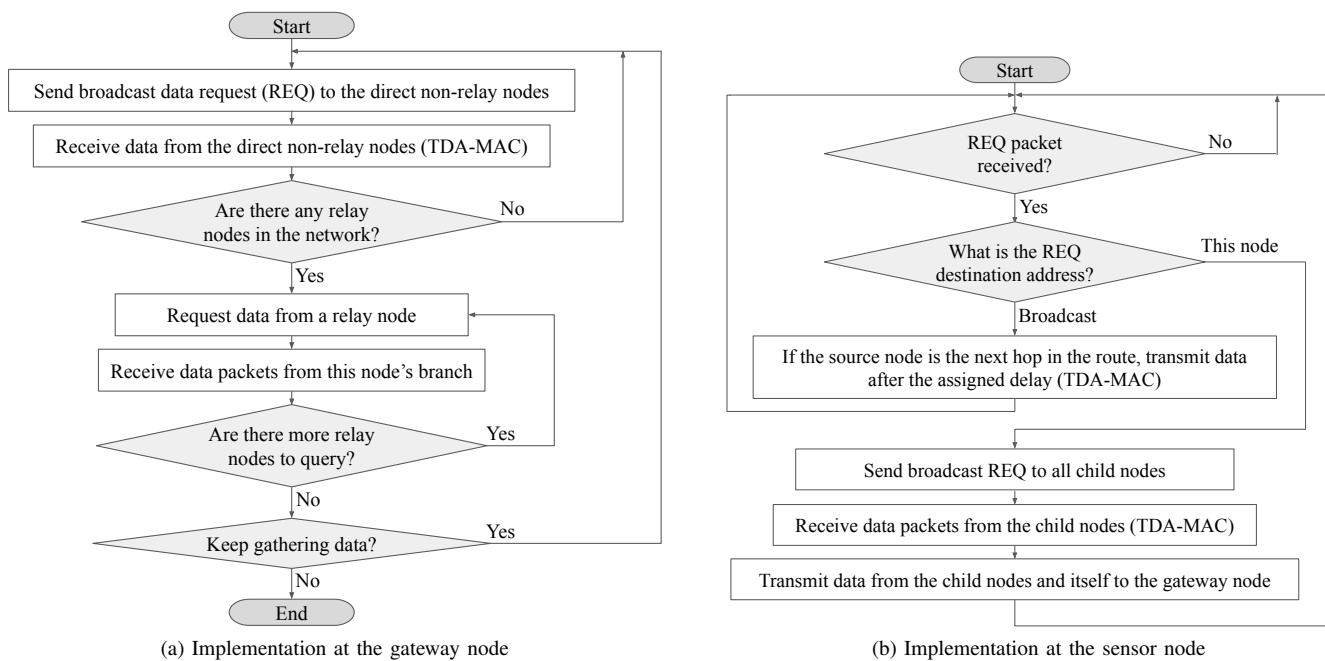


Fig. 5. Sequential Dual-Hop TDA-MAC transmission schedule. The gateway node first uses TDA-MAC to gather the data from the directly connected non-relay sensor nodes. It then gathers the data from all relay nodes sequentially. The relay nodes employ TDA-MAC to gather the data from their child nodes before transmitting it back to the gateway node.

to packet loss, since the timing of the upcoming REQ transmissions is independent of the number of data packets received at the gateway or the relay nodes. This process is explained below.

First, the expected duration of every instance of single-hop TDA-MAC, referred to as a "subframe", at the gateway node and at every relay node, is calculated by applying the TDA-MAC frame duration formula from (3):

$$\forall i \in \{1 \cup M_{\text{relays}}\},$$

$$\tau_{\text{sf}}[i] = \max_{\substack{n \in [2, N] \\ R[i, n] = 1}} \left\{ 2T_p[i, n] + T_{\text{tx}}[i, n] + \tau_{\text{dp}}[n] \right\} + \tau_{\text{rp}} \quad (23)$$

where  $\tau_{\text{sf}}[i]$  is the TDA-MAC subframe duration with node  $i$  as the master node (either gateway or relay),  $\tau_{\text{dp}}[n]$  is the duration of the data packet from node  $n$ , and  $\tau_{\text{rp}}$  is the duration of the REQ packet.

The relay nodes can then schedule their data transmissions back to the gateway node based on their knowledge of the subframe duration. For example, when the relay node  $i$  receives a unicast REQ packet asking it to gather the data within its network branch, it transmits a broadcast REQ packet to its child nodes and schedules its data transmission back to the gateway after a delay  $\tau_{\text{sf}}[i]$ . During this period, it receives the data packets from its child nodes. When this delay expires, it transmits its own data packet and forwards the data from its child nodes to the gateway node. In this way, the relay nodes follow a rigid, predictable schedule, independent of the data packet receptions.

The gateway node uses its knowledge of all subframe durations to schedule its next REQ packet transmission, which is either broadcast to all direct non-relay nodes or unicast to a particular relay node. For example, if the current REQ transmission is broadcast, the next REQ transmission

is scheduled after the following delay, allowing the sensor nodes just enough time to send back their data packets using TDA-MAC:

$$\tau_{\text{req}} = \tau_{\text{sf}}[1] + \tau_g \quad (24)$$

where  $\tau_g$  is a guard interval, e.g. 100 ms. After this delay, the gateway node proceeds with the SDH-TDA-MAC by sending out a REQ packet to the first relay node, asking it to gather and send back the data within its network branch, as shown in the flowchart in Fig. 5a.

After transmitting a unicast REQ packet to a relay node, e.g. node  $i$ , the gateway node schedules its next REQ transmission after the following delay:

$$\tau_{\text{req}} = \tau_{\text{sf}}[i] + 2T_p[1, i] + \left( \sum_{\substack{n \in [2, N] \\ R[i, n] = 1}} \tau_{\text{dp}}[n] \right) + \tau_{\text{dp}}[i] + \tau_{\text{rp}} + \tau_g \quad (25)$$

This delay allows enough time for the relay node  $i$  to receive the REQ packet, gather the data from its child nodes and relay the data packets, including sending its own, back to the gateway node. After this delay, the gateway node proceeds with the SDH-TDA-MAC by sending a REQ packet to the next relay node or transmitting a broadcast REQ packet again, if all relay nodes have been queried, as shown in the flowchart in Fig. 5a.

#### IV. SIMULATION RESULTS

In this section we evaluate our proposed SDH-TDA-MAC protocol using a BELLHOP [44] based Matlab simulation model of a large scale UASN that represents the type of network currently under development in the EPSRC USMART project [28] [34].

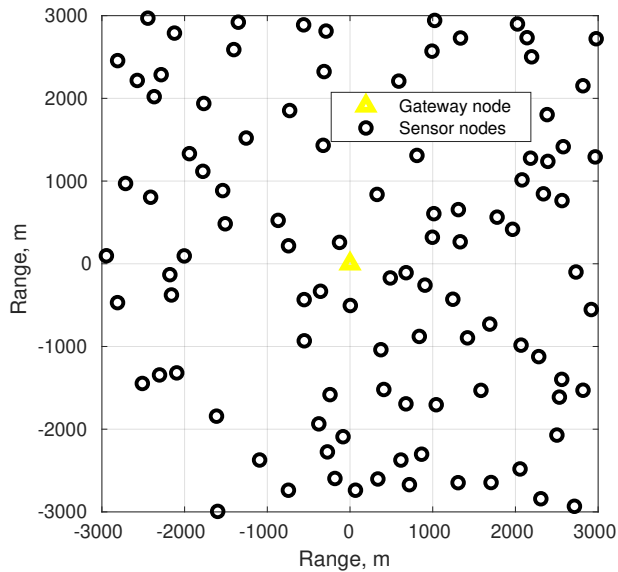


Fig. 6. Top view of the simulated network topology with 100 sensor nodes; depth of gateway node - 10 m, depth of sensor nodes - random between 470-490 m

### A. Simulation Setup

Table III describes the parameters of the Matlab model used for the simulation experiments in this paper. They correspond to a UASN data gathering scenario with 100 low cost, low specification sensor nodes deployed across a  $6 \times 6 \text{ km}^2$  area on the sea bed at 470-490 m depth, as depicted in Fig. 6.

We include a synchronization header (a unique waveform for detection and correlation at the receiver) in our packet model to reflect a typical structure of the low cost underwater acoustic modems, e.g. [47] [48]. The duration of the data packet in our simulation model is calculated as follows:

$$\tau_{dp} = \tau_{\text{header}} + \frac{N_{\text{bits}}}{D} = 50 + \frac{48 \times 8}{640} = 650 \text{ ms}, \quad (26)$$

where  $\tau_{dp}$  is the data packet duration,  $\tau_{\text{header}}$  is the header waveform duration,  $N_{\text{bits}} = 48 \times 8$  is the number of bits in a packet, and  $D = 640$  is the datarate in bits/s. The synchronization header also has an effect on the channel capacity, defined in this paper as the maximum achievable data throughput, i.e. if a constant stream of data packets was received at the gateway node without any gaps in time. It can be calculated by dividing the number of bits in a packet by the packet duration, thus yielding the maximum data rate achievable for this packet structure:

$$D_{\text{max}} = \frac{N_{\text{bits}}}{\tau_{dp}} = \frac{48 \times 8}{650} = 591 \text{ bits/s}, \quad (27)$$

which is lower than the modem bitrate of 640 bits/s due to the overhead caused by packet synchronization headers.

The channel between every pair of nodes was modelled using the BELLHOP ray tracing program [44], a well-established platform for simulating underwater acoustic wave propagation. We use the sound speed profile from the database provided by Dushaw [46], derived from the 2009 World Ocean Atlas temperature, pressure and salinity data in summer at (56.5°N, 11.5°W), i.e. in the North Atlantic

Ocean off the coast of the UK and Ireland. The sinusoidal surface and bottom profiles specified in Table III produce a more realistic scattering pattern of the multipath components, compared with a flat surface and bottom, due to the angles of incidence and reflection rapidly varying with range. This approach has been used in other works in the literature to simulate the small-scale roughness of sea surface/bottom, e.g. [49] [50].

For every source-receiver pair, the output of BELLHOP includes  $L$  echoes, each with a spreading loss  $a_{\text{spr}}[k]$ , propagation delay  $\tau_k$  and phase shift  $\theta_k$ . We then calculate the linear channel gain as follows:

$$G = \int_{f_{\text{min}}}^{f_{\text{max}}} \left| \sum_{k=1}^L a_{\text{spr}}[k] a_{\text{abs}}[k, f] e^{j(-2\pi f(\tau_k - \tau_0) + \theta_k)} \right|^2 df, \quad (28)$$

where  $f_{\text{min}}$  and  $f_{\text{max}}$  are the minimum and maximum frequency in the simulated channel,  $a_{\text{abs}}[k, f]$  is the absorption loss of the  $k^{\text{th}}$  echo at frequency  $f$  calculated using Thorp's formula [45], and  $\tau_0$  is the propagation delay of the first received echo. Crucially, this equation models the channel attenuation of wideband signals (the bandwidth spanning  $f_{\text{min}}$  to  $f_{\text{max}}$ ), expanding the single frequency simulation data produced by BELLHOP.

We use the following two performance metrics to quantify the network performance in terms of its data capacity and reliability, respectively:

- *Goodput* - data packet throughput at the gateway node, excluding duplicate packet transmissions.
- *Packet delivery ratio* - the ratio between the number of packets delivered to the gateway node (excluding duplicate packet transmissions) and the total number of packets generated by the sensor nodes.

To ensure statistical significance of the simulation results, all datapoints in the graphs presented in this section show an average of 50 simulations with different random seeds and node locations, with the error bars representing the 5th and 95th percentiles.

### B. Network Connectivity

Fig. 7 shows the improvement in network connectivity achieved by SDH-TDA-MAC, compared with the single-hop TDA-MAC protocol, i.e. extending the connectivity options of the sensor node from single-hop to dual-hop. A connection between any pair of nodes is considered to be present if the Signal-to-Noise Ratio (SNR) at the receiver is above the minimum threshold of 3 dB. The plot shows that the sensor nodes can afford to reduce their transmit power by approximately 16 dB to maintain full network connectivity via the dual-hop protocol, which can dramatically extend the battery life and reduce the cost of the sensor nodes. Although dual-hop communication requires more transmissions from the sensor nodes used as relays, compared with the single-hop setup, the increase in the number of transmissions is far smaller than by a factor of 40 (16 dB). Therefore, SDH-TDA-MAC achieves considerable overall energy savings, because the decrease in the transmit power is far greater than the increase in the number of transmissions. Fig. 7 also shows that even in scenarios where on average 50% of the sensor nodes are out of the gateway node's communication

TABLE III. SIMULATION PARAMETERS

Parameter	Value
Sensor node coverage area	6×6 km <sup>2</sup>
Number of nodes	100 (uniform random positions)
Sea depth	500 m
Surface node depth	10 m
Sensor node depth	Uniform random, 470-490 m
Frequency channel	24-28 kHz
Transmit power range	156-184 dB re $\mu\text{Pa}^2\text{m}^2$
Channel bitrate	640 bits/s
Packet size	Data: 48 bytes, REQ: 12 bytes
Synchronization header duration	50 ms
Sensor node packet traffic	Full buffer (maximum throughput data gathering scenario)
SNR threshold for reception	3 dB
Noise power	Ambient noise model [45], 10 m/s wind speed, 0.5 shipping activity factor
Channel model	Wideband multipath channel; impulse response data from BELLHOP [44]
Sound speed profile	Based on average summer data at (56.5°N, 11.5°W) [46]
Sea surface profile	Sinusoidal, 100 m wavelength, 5 m peak-to-peak depth
Sea bottom profile	Sinusoidal, 200 m interval, 10 m height

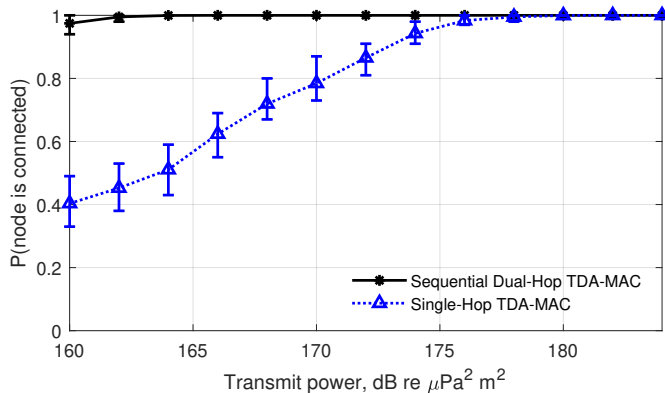


Fig. 7. Extending TDA-MAC from single-hop to dual-hop dramatically improves the probability of a node being connected and reduces the transmit power required to achieve full connectivity.

range (164 dB re  $\mu\text{Pa}^2\text{m}^2$  transmit power), such nodes can establish dual-hop links to achieve full connectivity, thus greatly improving network coverage.

### C. Network Goodput

Fig. 8 shows how the network goodput changes with transmit power, ranging from scenarios where approximately 40% of the nodes with a single-hop connection to the gateway node to a 100% single-hop topology. The results at transmit powers greater than 180 dB re  $\mu\text{Pa}^2\text{m}^2$  show that in a single-hop topology TDA-MAC performs highly efficiently and achieves 505 b/s goodput, 85% of the 591 b/s channel capacity.

This goodput loss is due to a purposely designed 100 ms guard interval ( $\approx 15\%$  of a data packet duration) between the

scheduled receptions. As the transmission power decreases, the SDH-TDA-MAC protocol is still able to achieve a high network goodput, especially considering the long propagation delays and the increasing number of dual-hop links (with duplicate packet transmissions not counting towards the goodput). For example, at 164 dB re  $\mu\text{Pa}^2\text{m}^2$  transmit power, when on average 50% of the nodes are connected via dual-hop links, the goodput is 308 bits/s, more than 50% of the channel capacity.

For comparison, Fig. 8 shows that the upper bound on the network goodput achievable by T-Lohi [51], a well-established contention-based MAC protocol designed for UASNs, is only 56 bits/s (9.5% of the channel capacity). Furthermore, this upper bound assumes a single contention round per data packet transmission, i.e. every single node is always successful in reserving a channel on its first try. In most realistic scenarios, especially with large numbers of nodes and medium to high traffic loads, this will not be the case, and the network goodput provided by T-Lohi will be far lower than the upper bound in Fig. 8 due to extended channel reservation periods caused by multiple nodes transmitting a tone in the same contention round.

Fig. 8 also compares the network goodput achieved by the SDH-TDA-MAC protocol with that provided by sequential polling, similar to UW-Polling [52] but optimized for our static scenario. It works similarly to the flowchart shown in Fig. 5, but instead of employing TDA-MAC, the gateway and relay nodes gather the data by sequentially polling their child nodes. The plot shows that using SDH-TDA-MAC instead of sequential polling significantly reduces the idle time on the channel and, thus, improves the network goodput by a factor of 2.6-5.2 in full network connectivity scenarios, i.e. with transmit power  $\geq 164$  dB re  $\mu\text{Pa}^2\text{m}^2$ .

These results show that the proposed protocol achieves

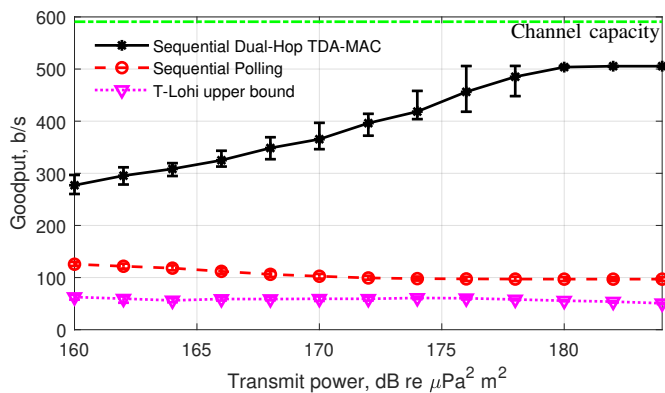


Fig. 8. Sequential Dual-Hop TDA-MAC achieves significantly higher network goodput, compared with T-Lohi and multi-hop sequential polling, by utilizing TDA-MAC for all many-to-one connections. The more single-hop nodes there are in the network, the higher the throughput gain is.

its primary purpose of enabling high throughput UASN deployments. In low throughput networks SDH-TDA-MAC is not as suitable as contention-based protocols due to the latency caused by the collision-free TDA-MAC frame structure, compared with the more flexible on-demand channel reservation approach, e.g. T-Lohi. However, the latency reduction afforded by such contention-based protocols can only be realized in low traffic load conditions, i.e. when a node is likely to reserve the channel without frequent contention from multiple other nodes. If the application layer traffic load exceeds the maximum supported network goodput, the latency will increase exponentially with increasing packet queues at the sensor nodes. Therefore, for high throughput scenarios considered in this paper, it is crucial to focus on the throughput/goodput as the primary performance metric.

#### D. Routing Redundancy with 10% Probability of Link Outage

In the rest of this section we evaluate the network performance under unreliable link conditions, i.e. when a proportion of transmissions fail due to random environmental factors, e.g. acoustic noise, multipath fading, signal path obstruction, etc. In particular, we investigate the effect of the routing diversity proposed in Subsection III-C on the network reliability under random link fading. Link fading was modelled using a classical two-state Markov process [53] to approximate large-scale underwater acoustic link fading often observed in practice, where link outage may last for tens of seconds or minutes due to changes in the channel caused by node movement or external factors, such as noise. In the two-state Markov model, both the duration of random link outage and the duration of normal link operation are exponentially distributed [54]. We fix the mean link outage duration at  $\tau_{\text{outage}} = 30$  s, whereas the mean duration of the normal link operation is calculated as follows [54]:

$$\tau_{\text{normal}} = \frac{1 - p_{\text{outage}}}{p_{\text{outage}}} \tau_{\text{outage}} \quad (29)$$

where  $p_{\text{outage}}$  is the probability of link outage.

Fig. 9 compares the packet delivery ratio, i.e. how many data packets were received at the gateway node vs how many packets were expected, at 10% probability of link outage, achieved by the SDH-TDA-MAC protocol with no route

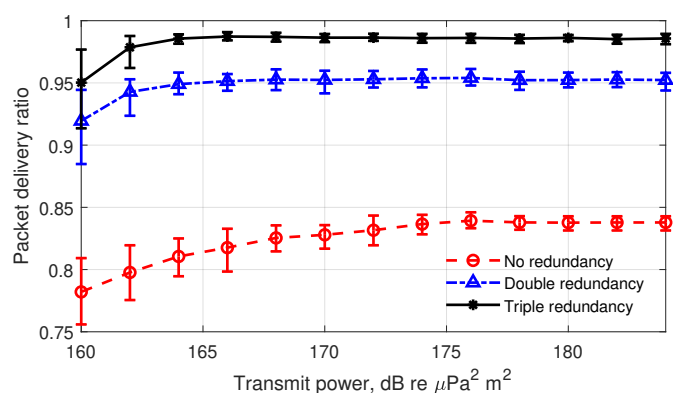


Fig. 9. Introducing double or triple routing redundancy into Sequential Dual-Hop TDA-MAC significantly increases the packet delivery ratio at the gateway node, due to an increased resilience of the network against random link failures at 10% probability of link outage.

diversity, and SDH-TDA-MAC with double and triple routing redundancies.

In full connectivity scenarios, i.e. at  $\geq 164$  dB re  $\mu\text{Pa}^2 \text{m}^2$  transmit power, the SDH-TDA-MAC protocol achieves between 81% and 84% packet delivery ratio, showing that the effect of the 10% probability of link outage accumulates across multiple hops and results in a greater than 10% end-to-end packet loss. For example, for a packet to be successfully delivered from a single-hop node, two consecutive transmissions must be successful - REQ packet from gateway to sensor node and data packet from sensor back to gateway node. In the case of dual-hop nodes, four consecutive transmissions must be successful - gateway-relay and relay-sensor REQ transmissions and sensor-relay, relay-gateway data transmissions. In contrast, by separating the channel reservation phase from the data transmission phase, contention-based protocols such as T-Lohi will perform more reliably than SDH-TDA-MAC, achieving a packet loss ratio roughly equal to the link outage probability, i.e. in this case the packet delivery ratio of approx. 90%. This shows that the high throughput performance of SDH-TDA-MAC comes at the cost of degradation in the network reliability. However, combining SDH-TDA-MAC with double or triple route diversity significantly reduces the cumulative effect of link failures, because for a packet to be successfully delivered, only one of two or three routes must be successful. Double routing redundancy increases the packet delivery ratio to 95-96% in full network connectivity scenarios, whereas adding another layer of redundancy further increases it to 98-99%, thus dramatically increasing the network reliability.

Fig. 10 examines the effect of routing redundancy on the network goodput. The plot shows that there is relatively little benefit in using high transmit power with routing redundancy, because the network goodput gain is relatively small. This is in contrast with the original SDH-TDA-MAC protocol without route diversity, which uses high throughput single-hop TDA-MAC to exploit the increasing number of direct sensor-to-gateway node connections. In SDH-TDA-MAC with route diversity all redundant routes are dual-hop; therefore, the number of direct non-relay nodes decreases and the number of relay nodes and dual-hop routes significantly increases. Nevertheless, the protocol achieves the goodput



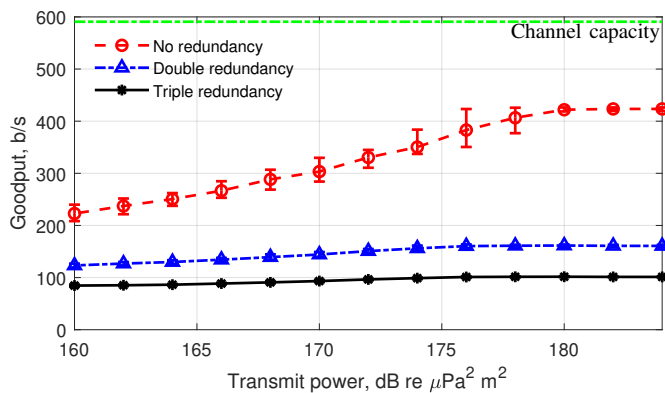


Fig. 10. Introducing double or triple routing redundancy into Sequential Dual-Hop TDA-MAC reduces the network goodput, but keeps it relatively flat against transmit power at 22-27% and 15-17% of the channel capacity, respectively, assuming 10% probability of link outage. Therefore, lower transmit power can be used for energy efficiency with little degradation in network goodput.

of 22-27% and 15-17% of the channel capacity at 10% probability of link outage, with double and triple routing redundancy respectively. These correspond to the MAC layer throughputs slightly higher than the 42% goodput at 164 dB re  $\mu\text{Pa}^2\text{m}^2$  transmit power achieved by the SDH-TDA-MAC protocol without redundancy, because the double/triple routing redundancy roughly doubles/triples the number of data transmissions in the network. Furthermore, the goodput achieved by our proposed protocol is still significantly higher than the upper bound of T-Lohi in Fig 8, despite the duplicate data packet overhead and 10% link outage probability.

### E. Network Tolerance Against Random Link Outage

Fig. 11 plots the packet delivery ratio at 168 dB re  $\mu\text{Pa}^2\text{m}^2$  transmit power against the probability of link outage. It is a useful way of determining how many random link failures a network can tolerate to meet a particular packet delivery ratio specification. For example, Fig. 11 shows that, if the UASN is required to guarantee 95% successful packet delivery, the SDH-TDA-MAC protocol without route diversity can only tolerate 2.5% random packet loss due to link failures. Whereas, to achieve the same specification, SDH-TDA-MAC with double or triple routing redundancy can tolerate random link outage of up to 10% or 17% respectively, which more realistically represent a real-world underwater acoustic channel, e.g. see [34]. This is a significant reliability improvement that justifies the overhead introduced by the routing redundancy. In the above example of the assured 95% packet delivery use case, by doubling the number of transmissions the network tolerance to random link fading increased 4 times, whereas tripling the number of transmissions increased this tolerance by a factor of  $\approx 7$ .

## V. CONCLUSION

The SDH-TDA-MAC protocol proposed in this paper facilitates efficient data gathering in UASNs via centralized dual-hop scheduling, but without the need for clock synchronization among the sensor nodes. BELLHOP-based simulations of a 100 node underwater sensor network revealed that SDH-TDA-MAC can achieve full network connectivity with 16 dB

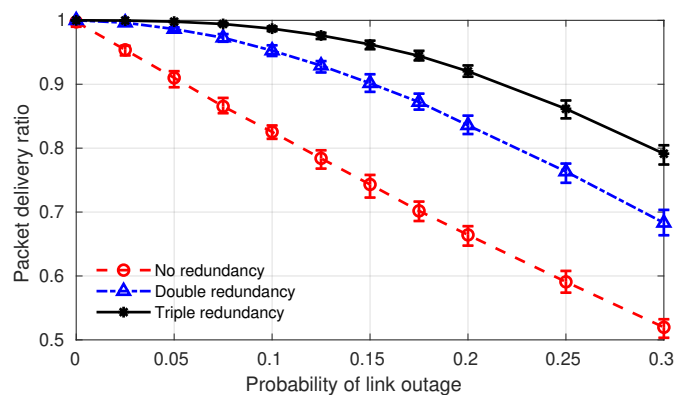


Fig. 11. The packet delivery ratio is significantly improved by combining Sequential Dual-Hop TDA-MAC with routing redundancy.

lower transmit power, compared with its single-hop counterpart, while still achieving network goodput in excess of 50% of the channel capacity, significantly higher than typical MAC protocols designed for UASNs. This is because of the spectral efficiency of TDA-MAC employed for all many-to-one connections at the gateway and relay nodes. Furthermore, SDH-TDA-MAC is designed not only for scenarios where a gateway node controls the data gathering traffic, but as a general collision-free MAC protocol for dual-hop networks with a single gateway node. It can support arbitrary sensor node initiated data traffic by using the downlink REQ packets for distributing a timing reference for every node's local transmission schedule.

Our proposed method of incorporating routing redundancy into the SDH-TDA-MAC protocol dramatically improves the network reliability at the cost of reducing the network goodput due to duplicate transmissions and an increased proportion of dual-hop links. For example, in an unreliable underwater acoustic communication channel with 10% probability of link outage, double routing redundancy increased the packet delivery ratio of SDH-TDA-MAC from 81-84% to 95-96%, and triple routing redundancy increased it to 98-99%, a vast improvement in network reliability, but at the cost of 100/200% data packet overhead and a corresponding drop in the network goodput. Incorporating the routing redundancy can dramatically increase the network tolerance against random link fading, given a particular reliability requirement. For example, to achieve a 95% packet delivery ratio, the network running SDH-TDA-MAC with double or triple routing redundancy can tolerate 10% or 17% random link fading respectively, compared with only 2.5% if no routing redundancy is used.

In conclusion, the high network goodput, low transmit power compared with the single-hop approach, no requirement for clock synchronization, and robust packet delivery via route diversity make SDH-TDA-MAC an efficient, reliable and practical approach to data gathering in UASNs.

## REFERENCES

[1] H. S. Dol, P. Casari, T. van der Zwan, and R. Otnes, "Software-defined underwater acoustic modems: Historical review and the NILUS approach," *IEEE Journal of Oceanic Engineering*, vol. 42, no. 3, pp. 722-737, 2017.



- [2] E. Demirors, G. Sklivanitis, G. E. Santagati, T. Melodia, and S. N. Batalama, "A high-rate software-defined underwater acoustic modem with real-time adaptation capabilities," *IEEE Access*, vol. 6, pp. 18 602–18 615, 2018.
- [3] C. Renner and A. Golkowski, "Acoustic modem for micro AUVs: Design and practical evaluation," in *Proceedings of ACM WUWNet'16*, 2016.
- [4] Y. Zakharov, B. Henson, R. Diamant, Y. Fei, P. Mitchell, N. Morozs, L. Shen, and T. Tozer, "Data packet structure and modem design for dynamic underwater acoustic channels," *IEEE Journal of Oceanic Engineering*, accepted (in press), Jul 2019.
- [5] E. Felemban, F. Shaikh, U. Qureshi, A. Sheikh, and S. Qaisar, "Underwater sensor network applications: A comprehensive survey," *International Journal of Distributed Sensor Networks*, vol. 11, no. 11, p. 896832, 2015.
- [6] B. Boom, J. He, S. Palazzo, P. Huang, C. Beyan, H.-M. Chou, F.-P. Lin, C. Spampinato, and R. Fisher, "A research tool for long-term and continuous analysis of fish assemblage in coral-reefs using underwater camera footage," *Ecological Informatics*, vol. 23, no. Supplement C, pp. 83 – 97, 2014.
- [7] A. K. Mohapatra, N. Gautam, and R. L. Gibson, "Combined routing and node replacement in energy-efficient underwater sensor networks for seismic monitoring," *IEEE Journal of Oceanic Engineering*, vol. 38, no. 1, pp. 80–90, 2013.
- [8] L. Lanbo, Z. Shengli, and C. Jun-Hong, "Prospects and problems of wireless communication for underwater sensor networks," *Wireless Communications and Mobile Computing*, vol. 8, no. 8, pp. 977–994, 2008.
- [9] J. Heidemann, M. Stojanovic, and M. Zorzi, "Underwater sensor networks: applications, advances and challenges," *Philosophical Transactions of the Royal Society of London A: Mathematical, Physical and Engineering Sciences*, vol. 370, no. 1958, pp. 158–175, 2012.
- [10] K. Chen, M. Ma, E. Cheng, F. Yuan, and W. Su, "A survey on MAC protocols for underwater wireless sensor networks," *IEEE Communications Surveys Tutorials*, vol. 16, no. 3, pp. 1433–1447, 2014.
- [11] N. Chirdchoo, W.-. Soh, and K. Chua, "Aloha-based MAC protocols with collision avoidance for underwater acoustic networks," in *Proceedings of IEEE INFOCOM'07*, pp. 2271–2275, 2007.
- [12] W. H. Liao and C. C. Huang, "SF-MAC: A spatially fair MAC protocol for underwater acoustic sensor networks," *IEEE Sensors Journal*, vol. 12, no. 6, pp. 1686–1694, 2012.
- [13] R. Diamant, P. Casari, F. Campagnaro, and M. Zorzi, "A handshake-based protocol exploiting the near-far effect in underwater acoustic networks," *IEEE Wireless Communications Letters*, vol. 5, no. 3, pp. 308–311, 2016.
- [14] M. Rahman, Y. Lee, and I. Koo, "An adaptive network allocation vector timer-based carrier sense multiple access with collision avoidance medium access control protocol for underwater acoustic sensor networks," *International Journal of Distributed Sensor Networks*, vol. 13, no. 1, 2017.
- [15] M. Molins and M. Stojanovic, "Slotted FAMA: a MAC protocol for underwater acoustic networks," in *Proceedings of IEEE OCEANS*, 2006.
- [16] Y. Noh, U. Lee, S. Han, P. Wang, D. Torres, J. Kim, and M. Gerla, "DOTS: A propagation delay-aware opportunistic MAC protocol for mobile underwater networks," *IEEE Transactions on Mobile Computing*, vol. 13, no. 4, pp. 766–782, 2014.
- [17] R. Zhao, H. Long, O. A. Dobre, X. Shen, T. M. N. Ngatched, and H. Mei, "Time reversal based MAC for multi-hop underwater acoustic networks," *IEEE Systems Journal*, Early Access, 2019.
- [18] P. Anjangi and M. Chitre, "Propagation-delay-aware unslotted schedules with variable packet duration for underwater acoustic networks," *IEEE Journal of Oceanic Engineering*, vol. 42, no. 4, pp. 977–993, Oct 2017.
- [19] R. Diamant and L. Lampe, "Spatial reuse time-division multiple access for broadcast ad hoc underwater acoustic communication networks," *IEEE Journal of Oceanic Engineering*, vol. 36, no. 2, pp. 172–185, 2011.
- [20] S. Lmai, M. Chitre, C. Laot, and S. Houcke, "Throughput-efficient super-TDMA MAC transmission schedules in ad hoc linear underwater acoustic networks," *IEEE Journal of Oceanic Engineering*, vol. 42, no. 1, pp. 156–174, 2017.
- [21] S. Lmai, M. Chitre, C. Laot., and S. Houcke, "Throughput-maximizing transmission schedules for underwater acoustic multihop grid networks," *IEEE Journal of Oceanic Engineering*, vol. 40, no. 4, pp. 853–863, 2015.
- [22] K. Kredo II, P. Djukic, and P. Mohapatra, "STUMP: Exploiting position diversity in the staggered TDMA underwater MAC protocol," in *Proceedings of IEEE INFOCOM*, 2009.
- [23] X. Zhuo, F. Qu, H. Yang, Y. Wei, Y. Wu, and J. Li, "Delay and queue aware adaptive scheduling-based MAC protocol for underwater acoustic sensor networks," *IEEE Access*, vol. 7, pp. 56 263–56 275, 2019.
- [24] N. Chirdchoo, W. Soh, and K. Chua, "MU-Sync: A time synchronization protocol for underwater mobile networks," in *Proceedings of ACM WUWNet'08*, 2008.
- [25] A. T. Gardner and J. A. Collins, "Advancements in high-performance timing for long term underwater experiments: A comparison of chip scale atomic clocks to traditional microprocessor-compensated crystal oscillators," in *Proceedings of IEEE OCEANS*, 2012.
- [26] K. Kebkal, O. Kebkal, E. Glushko, V. Kebkal, L. Sebastiao, A. Pascoal, J. Gomes, J. Ribeiro, H. Silva, M. Ribeiro, and G. Indivero, "Underwater acoustic modems with integrated atomic clocks for one-way travel-time underwater vehicle positioning," in *Proceedings of UACE'17*, 2017.
- [27] N. Morozs, P. Mitchell, and Y. Zakharov, "TDA-MAC: TDMA without clock synchronization in underwater acoustic networks," *IEEE Access*, vol. 6, pp. 1091–1108, 2018.
- [28] "EPSRC USMART (EP/P017975/1)," Mar 2018. [Online]. Available: <https://research.ncl.ac.uk/usmart/>
- [29] N. Morozs, P. Mitchell, and Y. Zakharov, "Linear TDA-MAC: Unsynchronized scheduling in linear underwater acoustic sensor networks," *IEEE Networking Letters*, Early Access, 2019.
- [30] G. Han, J. Jiang, N. Bao, L. Wan, and M. Guizani, "Routing protocols for underwater wireless sensor networks," *IEEE Communications Magazine*, vol. 53, no. 11, pp. 72–78, 2015.
- [31] S. Basagni, C. Petrioli, R. Petroccia, and D. Spaccini, "CARP: A channel-aware routing protocol for underwater acoustic wireless networks," *Ad Hoc Networks*, vol. 34, pp. 92 – 104, 2015.
- [32] M. Zorzi, P. Casari, N. Baldo, and A. F. Harris, "Energy-efficient routing schemes for underwater acoustic networks," *IEEE Journal on Selected Areas in Communications*, vol. 26, no. 9, pp. 1754–1766, 2008.
- [33] R. Otnes, J. Locke, A. Komulainen, S. Blouin, D. Clark, H. Austad, and J. Eastwood, "Dflood network protocol over commercial modems," in *Proceedings of IEEE UComms'18*, 2018.
- [34] N. Morozs, P. Mitchell, Y. Zakharov, R. Mourya, Y. Petillot, T. Gibney, M. Dragone, B. Sherlock, J. Neasham, C. Tsimenidis, M. Sayed, A. McConnell, S. Aracri, and A. Stokes, "Robust TDA-MAC for practical underwater sensor network deployment: Lessons from USMART sea trials," in *Proceedings of ACM WUWNet'18*, 2018.
- [35] A. Cho, C. Yun, Y.-K. Lim, and Y. Choi, "Asymmetric propagation delay-aware TDMA MAC protocol for mobile underwater acoustic sensor networks," *Applied Sciences*, vol. 8, no. 6, 2018.
- [36] M. Watfa, S. Selman, and H. Denkilian, "UW-MAC: An underwater sensor network mac protocol," *International Journal of Communication Systems*, vol. 23, no. 4, pp. 485–506, 2010.
- [37] R. Petroccia, "A distributed ID assignment and topology discovery protocol for underwater acoustic networks," in *Proceedings of IEEE UComms'16*, 2016.
- [38] A. K. Othman, A. E. Adams, and C. C. Tsimenidis, "Node discovery protocol and localization for distributed underwater acoustic networks," in *Proceedings of AICT-ICIW'06*, 2006.
- [39] N. Morozs, P. Mitchell, and Y. Zakharov, "Routing strategies for dual-hop TDA-MAC: Trade-off between network throughput and reliability," in *Proceedings of UACE'19*, 2019.

- [40] U. Feige, "A threshold of  $\ln N$  for approximating set cover," *J. ACM*, vol. 45, no. 4, pp. 634–652, 1998.
- [41] D. Hochbaum, "Approximation algorithms for the set covering and vertex cover problems," *SIAM J. Comput.*, vol. 11, pp. 555–556, 1980.
- [42] P. Slavík, "A tight analysis of the greedy algorithm for set cover," *Journal of Algorithms*, vol. 25, no. 2, pp. 237 – 254, 1997.
- [43] N. Morozs, P. Mitchell, and Y. Zakharov, "Unsynchronized dual-hop scheduling for practical data gathering in underwater sensor networks," in *Proceedings of IEEE UComms'18*, 2018.
- [44] M. Porter, "The BELLHOP manual and users guide: Preliminary draft," Jan 2011. [Online]. Available: <http://oalib.hlsresearch.com/Rays/HLS-2010-1.pdf>
- [45] M. Stojanovic, "On the relationship between capacity and distance in an underwater acoustic communication channel," *SIGMOBILE Mob. Comput. Commun. Rev.*, vol. 11, no. 4, pp. 34–43, 2007.
- [46] B. Dushaw. (2009) Worldwide sound speed, temperature, salinity, and buoyancy from the NOAA world ocean atlas. [Online]. Available: <http://staff.washington.edu/dushaw/WOA/>
- [47] J. A. Neasham, G. Goodfellow, and R. Sharphouse, "Development of the "Seatrac" miniature acoustic modem and USBL positioning units for subsea robotics and diver applications," in *Proceedings of IEEE OCEANS'15*, 2015.
- [48] B. Sherlock, J. A. Neasham, and C. C. Tsimenidis, "Spread-spectrum techniques for bio-friendly underwater acoustic communications," *IEEE Access*, vol. 6, pp. 4506–4520, 2018.
- [49] K. Belibassakis, "A coupled-mode model for the scattering of water waves by shearing currents in variable bathymetry," *Journal of Fluid Mechanics*, vol. 578, p. 413434, 2007.
- [50] S. M. Glenn, M. F. Crowley, D. B. Haidvogel, and Y. T. Song, "Underwater observatory captures coastal upwelling events off New Jersey," *Eos, Transactions American Geophysical Union*, vol. 77, no. 25, pp. 233–236, 1996.
- [51] A. A. Syed, W. Ye, and J. Heidemann, "Comparison and evaluation of the T-lohi MAC for underwater acoustic sensor networks," *IEEE Journal on Selected Areas in Communications*, vol. 26, no. 9, pp. 1731–1743, 2008.
- [52] F. Favaro, P. Casari, F. Guerra, and M. Zorzi, "Data upload from a static underwater network to an AUV: Polling or random access?" in *Proceedings of IEEE OCEANS*, 2012.
- [53] M. Zorzi, R. R. Rao, and L. B. Milstein, "On the accuracy of a first-order Markov model for data transmission on fading channels," in *Proceedings of IEEE ICUPC'95*, 1995.
- [54] E. N. Gilbert, "Capacity of a burst-noise channel," *The Bell System Technical Journal*, vol. 39, no. 5, pp. 1253–1265, 1960.



**Paul D. Mitchell** (M'00 - SM'09) received the M.Eng. and Ph.D. degrees from the University of York, UK, in 1999 and 2003, respectively. His Ph.D. research was on medium-access control for satellite systems, which was supported by British Telecom. He has been a member of the Department of Electronic Engineering, University of York, since 2002, and is currently a Reader. He has gained industrial experience at BT and QinetiQ. He has authored over 120 refereed journals and conference papers and has served on numerous international conference program committees. His current research interests include medium-access control and networking for underwater and mobile communication systems, and the application of artificial intelligence techniques to such problems. He is currently a Lead Investigator of EPSRC USMART and a Co-Investigator of EPSRC Full-Duplex projects. He was the General Chair of IEEE ISWCS which was held in York, in 2010, the Track Chair of IEEE VTC, in 2015, and TPC co-Chair in 2019. He is an Associate Editor of the IET Wireless Sensor Systems journal and the Sage International Journal.



**Nils Morozs** (S'13 - M'17) received the M.Eng. and Ph.D. degrees in electronic engineering from the University of York, in 2012 and 2015, respectively. His Ph.D. research was part of the EU FP7 ABSOLUTE Project where he developed LTE-compliant dynamic spectrum access methods for disaster relief and temporary event networks. Afterwards, he worked as a Researcher in Wi-Fi and wireless convergence at BT, Martlesham, UK, and a Research Associate in the area of HAP-based communications at the Department of Electronic Engineering, University of York. He is currently Research Associate at this Department, working on protocol design for underwater acoustic sensor networks as part of the EPSRC USMART project. His research interests include the development of protocols and architectures for wireless radio and acoustic networks.



**Yuriy Zakharov** (M'01 - SM'08) received the M.Sc. and Ph.D. degrees in electrical engineering from the Power Engineering Institute, Moscow, Russia, in 1977 and 1983, respectively. From 1977 to 1983, he was with the Special Design Agency in the Moscow Power Engineering Institute. From 1983 to 1999, he was with the N. N. Andreev Acoustics Institute, Moscow. From 1994 to 1999, he was with Nortel as a DSP Group Leader. Since 1999, he has been with the Communications Research Group, University of York, UK, where he is currently a Reader in the Department of Electronic Engineering. His research interests include signal processing, communications, and underwater acoustics.